Physics Letters B 733 (2014) 36–45

Contents lists available at ScienceDirect

Physics Letters B

www.elsevier.com/locate/physletb

A study of *CP* violation in $B^{\pm} \to DK^{\pm}$ and $B^{\pm} \to D\pi^{\pm}$ decays with $D \to K^0_S K^{\pm}\pi^{\mp}$ final states

LHCb Collaboration

ARTICLE INFO

Article history:
Received 12 February 2014
Received in revised form 26 March 2014
Accepted 26 March 2014
Available online 13 April 2014
Editor: L. Rolandi

ABSTRACT

A first study of *CP* violation in the decay modes $B^{\pm} \to [K^0_S K^{\pm}\pi^{\mp}]_D h^{\pm}$ and $B^{\pm} \to [K^0_S K^{\mp}\pi^{\pm}]_D h^{\pm}$, where h labels a K or π meson and D labels a D^0 or $\overline{D}{}^0$ meson, is performed. The analysis uses the LHCb data set collected in pp collisions, corresponding to an integrated luminosity of 3 fb^{-1}. The analysis is sensitive to the *CP*-violating CKM phase γ through seven observables: one charge asymmetry in each of the four modes and three ratios of the charge-integrated yields. The results are consistent with measurements of γ using other decay modes.

1. Introduction

A precise measurement of the unitarity triangle angle $\gamma = \arg(-\frac{V_{ud}V^*_{ub}}{V_{cd}V^*_{cb}})$ is one of the most important tests of the Cabibbo Kobayashi Maskawa (CKM) mechanism. This parameter can be accessed through measurements of observables in decays of charged B mesons to a neutral D meson and a kaon or pion, where D labels a D^0 or $\overline{D}{}^0$ meson decaying to a particular final state accessible to D^0 and $\overline{D}{}^0$. Such decays are sensitive to γ through the interference between $b \to c\bar{u}s$ and $b \to u\bar{c}s$ amplitudes. They offer an attractive means to measure γ because the effect of physics beyond the Standard Model is expected to be negligible, thus allowing interesting comparisons with other measurements where such effects could be larger.

The determination of γ using $B^{\pm} \to DK^{\pm}$ decays was first proposed for D decays to the *CP*-eigenstates K^+K^- and $\pi^+\pi^-$ (so-called "GLW" analysis) [1,2]. Subsequently, the analysis of the $K^{\pm}\pi^{\mp}$ final state was proposed (named "ADS") [3,4], where the suppression between the colour favoured $B^- \to D^0K^-$ and suppressed $B^- \to \overline{D}{}^0K^-$ decays is compensated by the CKM suppression of the $D^0 \to K^+\pi^-$ decay relative to $\overline{D}{}^0 \to K^+\pi^-$, resulting in large interference. The LHCb Collaboration has published the two-body ADS and GLW analyses [5], the Dalitz analysis of the decay $B^{\pm} \to [K^0_S h^{\pm}h^{\mp}]_D K^{\pm}$ $(h = \pi, K)$ [6] and the ADS-like analysis of the decay mode $B^{\pm} \to [K^{\pm}\pi^{\mp}\pi^{\pm}\pi^{\mp}]_D K^{\pm}$ [7], where $[X]_D$ indicates a given final state X produced by the decay of the D meson. These measurements have recently been combined to yield the result $\gamma = (72.0^{+14.7}_{-15.6})^\circ$ [8], which is in agreement with the results obtained by the BaBar and Belle Collaborations of $\gamma = (69^{+17}_{-16})^\circ$ [9] and $\gamma = (68^{+15}_{-14})^\circ$ [10], respectively. In analogy to studies in charged B meson decays, sensitivity to γ can also be gained from decays of neutral B mesons, as has been demonstrated in the LHCb analysis of $B^0 \to [K^+K^-]_D K^{*0}$ decays [11].

The inclusion of additional $B^{\pm} \to DK^{\pm}$ modes can provide further constraints on γ. In this Letter, an analysis of the $D \to K^0_S K^{\pm}\pi^{\mp}$ final states is performed, the first ADS-like analysis to use singly Cabibbo-suppressed (SCS) decays. The two decays, $B^{\pm} \to [K^0_S K^{\pm}\pi^{\mp}]_D h^{\pm}$ and $B^{\pm} \to [K^0_S K^{\mp}\pi^{\pm}]_D h^{\pm}$, are distinguished by the charge of the $K^{\pm}$ from the decay of the D meson relative to the charge of the B meson, so that the former is labelled "same sign" (SS) and the latter "opposite sign" (OS).

In order to interpret *CP*-violating effects using these three-body decays it is necessary to account for the variation of the D decay strong phase over its Dalitz plot due to the presence of resonances between the particles in the final state. Instead of employing an amplitude model to describe this phase variation, direct measurements of the phase made by the CLEO Collaboration are used, which are averaged over large regions of the Dalitz plot [12]. The same CLEO study indicates that this averaging can be employed without a large loss of sensitivity. The use of the CLEO results avoids the need to introduce a systematic uncertainty resulting from an amplitude model description.

The analysis uses the full 2011 and 2012 LHCb pp collision data sets, corresponding to integrated luminosities of 1 and 2 fb^{-1} and centre-of-mass energies of $\sqrt{s} = 7$ TeV and 8 TeV, respectively. The results are measurements of *CP*-violating observables that can be interpreted in terms of γ and other hadronic parameters of the $B^{\pm}$ meson decay.

http://dx.doi.org/10.1016/j.physletb.2014.03.051

2. Formalism

The SS decay $B^+ \to [K^0_S K^+\pi^-]_D K^+$ can proceed via a D^0 or $\overline{D}{}^0$ meson, so that the decay amplitude is the sum of two amplitudes that interfere,

$$A\big(m^2_{K^0_S K}, m^2_{K^0_S \pi}\big) = A_{\overline{D}{}^0}\big(m^2_{K^0_S K}, m^2_{K^0_S \pi}\big) + r_B e^{i(\delta_B+\gamma)} A_{D^0}\big(m^2_{K^0_S K}, m^2_{K^0_S \pi}\big), \quad (1)$$

where $A_{\{D^0,\overline{D}{}^0\}}(m^2_{K^0_S K}, m^2_{K^0_S \pi})$ are the D^0 and $\overline{D}{}^0$ decay amplitudes to a specific point in the $K^0_S K^+\pi^-$ Dalitz plot. The amplitude ratio r_B is $\frac{|A(B^+\to D^0K^+)|}{|A(B^+\to \overline{D}{}^0K^+)|} = 0.089 \pm 0.009$ [8] and δ_B is the strong phase difference between the $B^+ \to D^0K^+$ and $B^+ \to \overline{D}{}^0K^+$ decays. The calculation of the decay rate in a region of the Dalitz plot requires the evaluation of the integral of the interference term between the two D decay amplitudes over that region. Measurements have been made by the CLEO Collaboration [12], where quantum-correlated D decays are used to determine the integral of the interference term directly in the form of a "coherence factor", $\kappa_{K^0_S K\pi}$, and an average strong phase difference, $\delta_{K^0_S K\pi}$, as first proposed in Ref. [13]. The coherence factor can take a value between 0 and 1 and is defined through the expression

$$\kappa_{K^0_S K\pi} e^{-i\delta_{K^0_S K\pi}} \equiv \frac{\int A^*_{K^0_S K^-\pi^+}(m^2_{K^0_S K}, m^2_{K\pi}) A_{K^0_S K^+\pi^-}(m^2_{K^0_S K}, m^2_{K\pi}) dm^2_{K^0_S K} dm^2_{K\pi}}{A^{\text{int.}}_{K^0_S K^-\pi^+} A^{\text{int.}}_{K^0_S K^+\pi^-}}, \quad (2)$$

where $A^{\text{int.}}_{K^0_S K^\pm\pi^\mp} = \int |A_{K^0_S K^\pm\pi^\mp}(m^2_{K^0_S K}, m^2_{K\pi})|^2 dm^2_{K^0_S K} dm^2_{K\pi}$. This avoids the significant modelling uncertainty incurred by the determination of the strong phase difference between the D^0 and $\overline{D}{}^0$ amplitudes at each point in the Dalitz region from an amplitude model. The decay rates, Γ, to the four final states can therefore be expressed as

$$\begin{aligned}\Gamma^\pm_{\text{SS},DK} &= z\big[1 + r_B^2 r_D^2 + 2r_B r_D \kappa_{K^0_S K\pi} \cos(\delta_B \pm \gamma - \delta_{K^0_S K\pi})\big] \\ \Gamma^\pm_{\text{OS},DK} &= z\big[r_B^2 + r_D^2 + 2r_B r_D \kappa_{K^0_S K\pi} \cos(\delta_B \pm \gamma + \delta_{K^0_S K\pi})\big] \end{aligned} \quad (3)$$

where r_D is the amplitude ratio for $D^0 \to K^0_S K^+\pi^-$ with respect to $D^0 \to K^0_S K^-\pi^+$ and z is the normalisation factor. Analogous equations can be written for the $B^\pm \to D\pi^\pm$ system, with r_B^π and δ_B^π replacing r_B and δ_B, respectively. Less interference is expected in the $B^\pm \to D\pi^\pm$ system where the value of r_B^π is much lower, approximately 0.015 [8]. These expressions receive small corrections from mixing in the charm system which, though accounted for in Section 7, are not explicitly written here. At the current level of precision these corrections have a negligible effect on the final results.

Observables constructed using the decay rates in Eq. (3) have a sensitivity to γ that depends upon the value of the coherence factor, with a higher coherence corresponding to greater sensitivity. The CLEO Collaboration measured the coherence factor and average strong phase difference in two regions of the Dalitz plot: firstly across the whole Dalitz plot, and secondly within a region ± 100 MeV/c^2 around the $K^*(892)^\pm$ resonance, which decays to $K^0_S\pi^\pm$, where, though the sample size is diminished, the coherence is higher. The measured values are $\kappa_{K^0_S K\pi} = 0.73 \pm 0.08$ and $\delta_{K^0_S K\pi} = 8.3 \pm 15.2^\circ$ for the whole Dalitz plot, and $\kappa_{K^0_S K\pi} = 1.00 \pm 0.16$ and $\delta_{K^0_S K\pi} = 26.5 \pm 15.8^\circ$ in the restricted region. The branching fraction ratio of $D^0 \to K^0_S K^+\pi^-$ to $D^0 \to K^0_S K^-\pi^+$ decays was found to be 0.592 ± 0.044 in the whole Dalitz plot and 0.356 ± 0.034 in the restricted region [12].

Eight yields are measured in this analysis, from which seven observables are constructed. The charge asymmetry is measured in each of the four decay modes, defined as $\mathcal{A}_{\text{SS},DK} \equiv \frac{N^{DK^-}_{SS} - N^{DK^+}_{SS}}{N^{DK^-}_{SS} + N^{DK^+}_{SS}}$ for the $B^\pm \to [K^0_S K^\pm\pi^\mp]_D K^\pm$ mode and analogously for the other modes. The ratios of $B^\pm \to DK^\pm$ and $B^\pm \to D\pi^\pm$ yields are determined for the SS and OS decays, $\mathcal{R}_{DK/D\pi,\text{SS}}$ and $\mathcal{R}_{DK/D\pi,\text{OS}}$ respectively, and the ratio of SS to OS $B^\pm \to D\pi^\pm$ yields, $\mathcal{R}_{\text{SS/OS}}$, is measured. The measurements are performed both for the whole D Dalitz plot and in the restricted region around the $K^*(892)^\pm$ resonance.

3. The LHCb detector and data set

The LHCb detector [14] is a single-arm forward spectrometer covering the pseudorapidity range $2 < \eta < 5$, designed for the study of particles containing b or c quarks. The detector includes a high-precision tracking system consisting of a silicon-strip vertex detector surrounding the pp interaction region, a large-area silicon-strip detector located upstream of a dipole magnet with a bending power of about 4 Tm, and three stations of silicon-strip detectors and straw drift tubes placed downstream. The combined tracking system provides a momentum measurement with relative uncertainty that varies from 0.4% at 5 GeV/c to 0.6% at 100 GeV/c, and impact parameter (IP) resolution of 20 μm for tracks with large transverse momentum. Different types of charged hadrons are distinguished by particle identification (PID) information from two ring-imaging Cherenkov (RICH) detectors [15]. Photon, electron and hadron candidates are identified by a calorimeter system consisting of scintillating-pad and preshower detectors, an electromagnetic calorimeter and a hadronic calorimeter. Muons are identified by a system composed of alternating layers of iron and multiwire proportional chambers.

The trigger consists of a hardware stage, based on information from the calorimeter and muon systems, followed by a software stage, which applies a full event reconstruction. The software trigger searches for a track with large p_T and large IP with respect to any pp interaction point, also called a primary vertex (PV). This track is then required to be part of a two-, three- or four-track secondary vertex with a high p_T sum, significantly displaced from any PV. A multivariate algorithm [16] is used for the identification of secondary vertices consistent with the decay of a b hadron.

Samples of around two million $B^\pm \to [K^0_S K^\mp\pi^\pm]_D\pi^\pm$ and two million $B^\pm \to [K^0_S K^\mp\pi^\pm]_D K^\pm$ decays are simulated to be used in the analysis, along with similarly-sized samples of $B^\pm \to [K^0_S\pi^+\pi^-]_D\pi^\pm$, $B^\pm \to [K^0_S K^+K^-]_D\pi^\pm$ and $B^\pm \to [K^\pm\pi^\mp\pi^+\pi^-]_D\pi^\pm$ decays that are used to study potential backgrounds. In the simulation, pp collisions are generated using Pythia [17] with a specific LHCb configuration [18]. Decays of hadronic particles are described by EvtGen [19], in which final state radiation is generated using Photos [20]. The interaction of the generated particles with the detector and its response are implemented using the Geant4 toolkit [21] as described in Ref. [22].

4. Candidate selection

Candidate $B \to [K^0_S K^\pm\pi^\mp]_D K$ and $B \to [K^0_S K^\pm\pi^\mp]_D\pi$ decays are reconstructed in events selected by the trigger and then the candidate momenta are refit, constraining the masses of the neutral D and K^0_S mesons to their known values [23] and the $B^\pm$ meson to originate from the primary vertex [24]. Candidates where the K^0_S decay is reconstructed using "long" pion tracks, which

leave hits in the VELO and downstream tracking stations, are analysed separately from those reconstructed using "downstream" pion tracks, which only leave hits in tracking stations beyond the VELO. The signal candidates in the former category are reconstructed with a better invariant mass resolution.

The reconstructed masses of the D and K^0_S mesons are required to be within 25 MeV/c^2 and 15 MeV/c^2, respectively, of their known values. Candidate $B^\pm \to DK^\pm$ decays are separated from $B^\pm \to D\pi^\pm$ decays by using PID information from the RICH detectors. A boosted decision tree (BDT) [25,26] that has been developed for the analysis of the topologically similar decay mode $B^\pm \to [K^0_S h^+ h^-]_D h'^\pm$ is applied to the reconstructed candidates. The BDT was trained using simulated signal decays, generated uniformly over the D^0 Dalitz plot, and background candidates taken from the $B^\pm$ invariant mass region in data between 5700 and 7000 MeV/c^2. It exploits the displacement of tracks from the decays of long-lived particles with respect to the PV through the use of $\chi^2_{\rm IP}$ variables, where $\chi^2_{\rm IP}$ is defined as the difference in χ^2 of a given PV fit with and without the considered track. The BDT also employs the $B^\pm$ and D candidate momenta, an isolation variable sensitive to the separation of the tracks used to construct the $B^\pm$ candidate from other tracks in the event, and the χ^2 per degree of freedom of the decay refit. In addition to the requirement placed on the BDT response variable, each composite candidate is required to have a vector displacement of production and decay vertices that aligns closely to its reconstructed momenta. The cosine of the angle between the displacement and momentum vectors is required to be less than 0.142 rad for the K^0_S and D^0 candidates, and less than 0.0141 rad (0.0100 rad) for long (downstream) $B^\pm$ candidates.

Additional requirements are used to suppress backgrounds from specific processes. Contamination from B decays that do not contain an intermediate D meson is minimised by placing a minimum threshold of 0.2 ps on the decay time of the D candidate. A potential background could arise from processes where a pion is misidentified as a kaon or vice versa. One example is the relatively abundant mode $B^\pm \to [K^0_S\pi^+\pi^-]_D h^\pm$, which has a branching fraction around ten times larger than the signal. These are suppressed by placing requirements on both the D daughter pion and kaon, making use of PID information. For K^0_S candidates formed from long tracks, the flight distance χ^2 of the candidate is used to suppress background from $B^\pm \to [K^\pm\pi^\mp\pi^+\pi^-]_D h^\pm$ decays. Where multiple candidates are found belonging to the same event, the candidate with the lowest value of the refit χ^2 per degree of freedom is retained and any others are discarded, leading to a reduction in the sample size of approximately 0.3%.

The $B^\pm$ invariant mass spectra are shown in Fig. 1 for candidates selected in the whole D Dalitz plot, overlaid with a parametric fit described in Section 5. The D Dalitz plots are shown in Fig. 2 for the $B^\pm \to DK^\pm$ and $B^\pm \to D\pi^\pm$ candidates that fall within a nominal $B^\pm$ signal region in $B^\pm$ invariant mass (5247–5317 MeV/c^2). The dominant $K^*(892)^\pm$ resonance is clearly visible within a horizontal band, and the window around this resonance used in the analysis is indicated.

5. Invariant mass fit

In order to determine the signal yields in each decay mode, simultaneous fits are performed to the $B^\pm$ invariant mass spectra in the range 5110 MeV/c^2 to 5800 MeV/c^2 in the different modes, both for candidates in the whole D Dalitz plot, and for only those inside the restricted region around the $K^*(892)^\pm$ resonance. The data samples are split according to the year in which the data were taken, the decay mode, the K^0_S type and the charge of the B candidate. The fit is parameterised in terms of the observables described in Section 2, rather than varying each signal yield in each category independently.

The probability density function (PDF) used to model the signal component is a modified Gaussian function with asymmetric tails, where the unnormalised form is given by

$$f(m; m_0, \alpha_L, \alpha_R, \sigma) \equiv \begin{cases} \exp[-(m-m_0)^2/(2\sigma^2 + \alpha_L(m-m_0)^2)] & \text{for } m < m_0, \\ \exp[-(m-m_0)^2/(2\sigma^2 + \alpha_R(m-m_0)^2)] & \text{for } m > m_0, \end{cases} \quad (4)$$

where m is the reconstructed mass, m_0 is the mean B mass and σ determines the width of the function. The $\alpha_{L,R}$ parameters govern the shape of the tail. The mean B mass is shared among all categories but is allowed to differ according to the year in which the data were collected. The α_L parameters are fixed to the values determined in the earlier analysis of $B^\pm \to [K^0_S\pi^+\pi^-]_D h^\pm$ [6]. The α_R parameters are common to the $B^\pm \to D\pi^\pm$ and $B^\pm \to DK^\pm$, SS and OS categories, and are allowed to vary in the fit. Only the width parameters $\sigma(B^\pm \to DK^\pm)$ are allowed to vary in the fit. The ratios $\sigma(B^\pm \to D\pi^\pm)/\sigma(B^\pm \to DK^\pm)$ are fixed according to studies of the similar mode $B^\pm \to [K^0_S\pi^+\pi^-]_D h^\pm$. The fitted values for $\sigma(B^\pm \to DK^\pm)$ vary by less than 10% around 14 MeV/c^2. The total yield of $B^\pm \to D\pi^\pm$ decays is allowed to vary between the different K^0_S type and year categories. The yields in the various D decay modes and different charges, and all the $B^\pm \to DK^\pm$ yields, are determined using the observables described in Section 2, rather than being fitted directly.

In addition to the signal PDF, two background PDFs are required. The first background PDF models candidates formed from random combinations of tracks and is represented by a linear function. In the fit within the restricted Dalitz region, where the sample size is significantly smaller, the slope of the linear function fitting the $B^\pm \to D\pi^\pm$ data is fixed to the value determined in the fit to the whole Dalitz plot. The second background PDF accounts for contamination from partially reconstructed processes. Given that the contamination is dominated by those processes that involve a real $D^0 \to K^0_S K^\pm\pi^\mp$ decay, the PDF is fixed to the shape determined from the more abundant mode $B^\pm \to [K^\pm\pi^\mp]_D h^\pm$. The yields of both these background components are free to vary in each data category.

A further significant background is present in the $B^\pm \to DK^\pm$ samples due to $\pi \to K$ misidentification of the much more abundant $B^\pm \to D\pi^\pm$ mode. This background is modelled in the $B^\pm \to DK^\pm$ spectrum using a Crystal Ball function [27], where the parameters of the function are common to all data categories in the fit and are allowed to vary. The yield of the background in the $B^\pm \to DK^\pm$ samples is fixed with respect to the fitted $B^\pm \to D\pi^\pm$ signal yield using knowledge of the RICH particle identification efficiencies that is obtained from data using samples of $D^{*\pm} \to [K\pi]_D\pi^\pm$ decays. The efficiency for kaons to be selected is found to be around 84% and the misidentification rate for pions is around 4%.

Production and detection asymmetries are accounted for, following the same procedure as in Refs. [5,7]. Values for the $B^\pm$ production and K detection asymmetries are assigned such that the combination of production and detection asymmetries corresponds to the raw asymmetry observed in $B^\pm \to J/\psi K^\pm$ decays [28]. The detection asymmetry assigned is $-0.5 \pm 0.7\%$ for each unit of strangeness in the final state to account for the differing interactions of K^+ and K^- mesons with the detector material. An analogous asymmetry is present for pions, though it is expected to be much smaller, and the detection asymmetry assigned is $0.0 \pm 0.7\%$. Any potential asymmetry arising from a difference between the responses of the left and right sides of the detector is minimised by

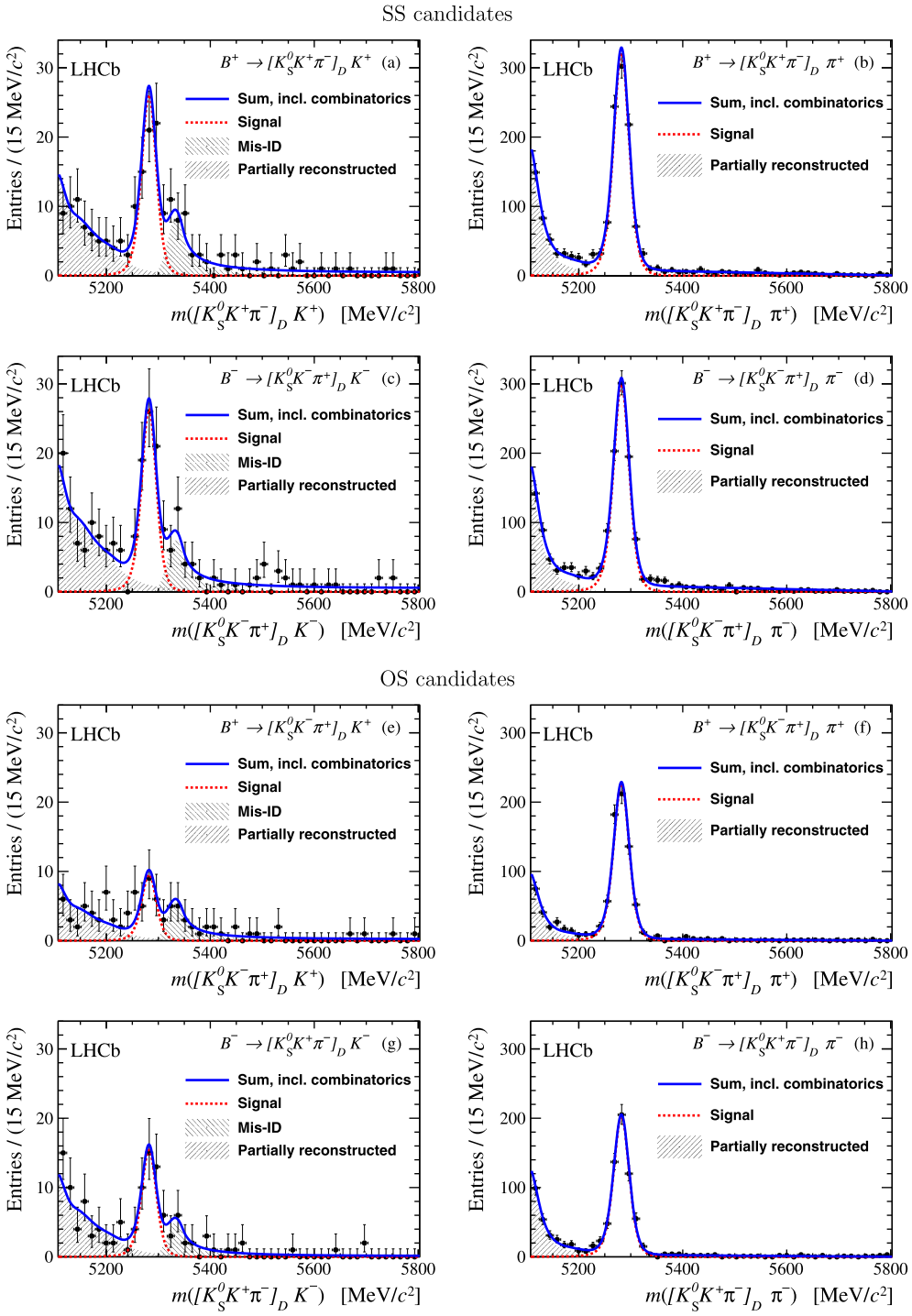

Fig. 1. Distributions of $B^{\pm}$ invariant mass of the SS and OS samples for the (a, c, e, g) $B^{\pm} \to DK^{\pm}$ and (b, d, f, h) $B^{\pm} \to D\pi^{\pm}$ candidates in the full data sample. The fits are shown for (a, b, e, f) B^{+} and (c, d, g, h) B^{-} candidates. Fit PDFs are superimposed.

combining approximately equal data sets taken with opposite magnet polarity.

A further correction is included to account for non-uniformities in the acceptance over the Dalitz plot. This efficiency correction primarily affects the $\mathcal{R}_{\mathrm{SS/OS}}$ observable, given the difference in the Dalitz distributions for the two D meson decay modes. A correction factor, ζ, is found by combining the LHCb acceptance, extracted from the simulated signal sample, and amplitude models, $A_{\mathrm{SS,OS}}(m^2_{K^0_S K}, m^2_{K^0_S \pi})$, for the Dalitz distributions of the SS or OS decays,

$$\zeta \equiv \frac{\int_{\mathcal{D}} \mathrm{d}m^2_{K^0_S K}\mathrm{d}m^2_{K^0_S \pi}[\epsilon(m^2_{K^0_S K}, m^2_{K^0_S \pi}) \times |A_{\mathrm{OS}}(m^2_{K^0_S K}, m^2_{K^0_S \pi})|^2]}{\int_{\mathcal{D}} \mathrm{d}m^2_{K^0_S K}\mathrm{d}m^2_{K^0_S \pi}[\epsilon(m^2_{K^0_S K}, m^2_{K^0_S \pi}) \times |A_{\mathrm{SS}}(m^2_{K^0_S K}, m^2_{K^0_S \pi})|^2]}, \tag{5}$$

where $\epsilon(m^2_{K^0_S K}, m^2_{K^0_S \pi})$ is the efficiency at a point in the Dalitz plot. The typical deviation of ζ from unity is found to be around 5%. The acceptance is illustrated in Fig. 3, where bins of variable size are used to ensure that statistical fluctuations due to the finite size of the simulated sample are negligible. The Dalitz distributions are

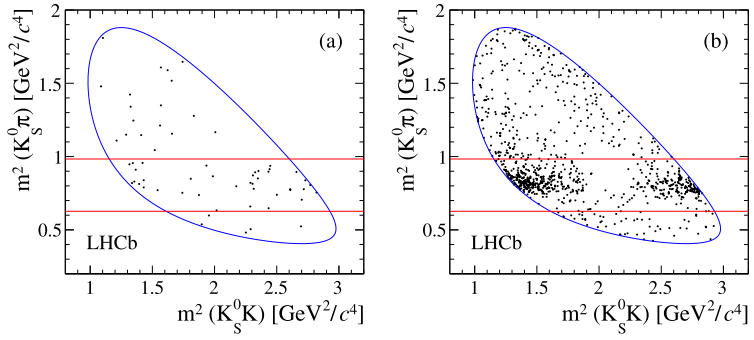

Fig. 2. Dalitz plot distribution of candidates selected in (a) the $B^\pm \to [K^0_S K\pi]_D K^\pm$ and (b) the $B^\pm \to [K^0_S K\pi]_D \pi^\pm$ decay modes, where the data in the SS and OS modes, and the two K^0_S categories, are combined. Candidates included are required to have a refitted $B^\pm$ mass in a nominal signal window between 5247 MeV/c^2 and 5317 MeV/c^2. The kinematic boundary is added in blue, and the restricted region around the $K^*(892)^\pm$ resonance is indicated by horizontal red lines. (For interpretation of the references to colour in this figure legend, the reader is referred to the web version of this article.)

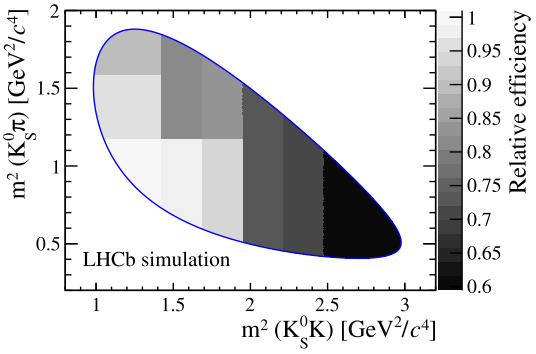

Fig. 3. Dalitz acceptance determined using simulated events and normalised relative to the maximum efficiency.

determined using the fact that little interference is expected in $B^\pm \to D\pi^\pm$ decays and, therefore, the flavour of the D meson is effectively tagged by the charge of the pion. In this case, the Dalitz distributions are given by considering the relevant D^0 decay ($D^0 \to K^0_S K^-\pi^+$ for SS and $D^0 \to K^0_S K^+\pi^-$ for OS). These D^0 decay Dalitz distributions are known and amplitude models from CLEO are available [12] from which the Dalitz distributions can be extracted.

Due to the restricted sample size under study, small biases exist in the determination of the observables. The biases are determined by generating and fitting a large number of simulated samples using input values obtained from the fit to data, and are typically found to be around 2%. The fit results are corrected accordingly.

The fit projections, with long and downstream K^0_S-type categories merged and 2011 and 2012 data combined, are given for the fit to the whole Dalitz plot in Fig. 1. The signal purity in a nominal mass range from 5247 MeV/c^2 to 5317 MeV/c^2 is around 85% for the $B^\pm \to DK^\pm$ samples and 96% for the $B^\pm \to D\pi^\pm$ samples. The signal yields derived from the fits to both the whole and restricted region of the Dalitz plot are given in Table 1. The fitted values of the observables are given in Table 2, including their systematic uncertainties as discussed in Section 6. The only significant difference between the observables fitted in the two regions is for the value of $\mathcal{R}_{SS/OS}$. This ratio is expected to differ significantly, given that the fraction of $D^0 \to K^0_S K^-\pi^+$ decays that are expected to lie inside the restricted portion of the Dalitz plot is around 75%, whereas for $D^0 \to K^0_S K^+\pi^-$ the fraction is around 44% [12]. This accounts for the higher value of $\mathcal{R}_{SS/OS}$ in the restricted region. The ratios between the $B^\pm \to DK^\pm$ and $B^\pm \to D\pi^\pm$ yields are consistent with that measured in the LHCb analysis of $B^\pm \to [K\pi]_D h^\pm$, $0.0774 \pm 0.0012 \pm 0.0018$ [5]. The CP asymmetries are consistent with zero in the $B^\pm \to D\pi^\pm$ system,

Table 1
Signal yields and their statistical uncertainties derived from the fit to the whole Dalitz plot region, and in the restricted region of phase space around the $K^*(892)^\pm$ resonance.

Mode	Whole Dalitz plot		$K^*(892)^\pm$ region	
	$DK^\pm$	$D\pi^\pm$	$DK^\pm$	$D\pi^\pm$
SS	145 ± 15	1841 ± 47	97 ± 12	1365 ± 38
OS	71 ± 10	1267 ± 37	26 ± 6	553 ± 24

Table 2
Results for the observables measured in the whole Dalitz plot region, and in the restricted region of phase space around the $K^*(892)^\pm$ resonance. The first uncertainty is statistical and the second is systematic. The corrections for production and detection asymmetries are applied, as is the efficiency correction defined in Eq. (5).

Observable	Whole Dalitz plot	$K^*(892)^\pm$ region
$\mathcal{R}_{SS/OS}$	$1.528 \pm 0.058 \pm 0.025$	$2.57 \pm 0.13 \pm 0.06$
$\mathcal{R}_{DK/D\pi,SS}$	$0.092 \pm 0.009 \pm 0.004$	$0.084 \pm 0.011 \pm 0.003$
$\mathcal{R}_{DK/D\pi,OS}$	$0.066 \pm 0.009 \pm 0.002$	$0.056 \pm 0.013 \pm 0.002$
$\mathcal{A}_{SS,DK}$	$0.040 \pm 0.091 \pm 0.018$	$0.026 \pm 0.109 \pm 0.029$
$\mathcal{A}_{OS,DK}$	$0.233 \pm 0.129 \pm 0.024$	$0.336 \pm 0.208 \pm 0.026$
$\mathcal{A}_{SS,D\pi}$	$-0.025 \pm 0.024 \pm 0.010$	$-0.012 \pm 0.028 \pm 0.010$
$\mathcal{A}_{OS,D\pi}$	$-0.052 \pm 0.029 \pm 0.017$	$-0.054 \pm 0.043 \pm 0.017$

where the effect of interference is expected to be small. The asymmetries in the $B^\pm \to DK^\pm$ system, $\mathcal{A}_{SS,DK}$ and $\mathcal{A}_{OS,DK}$, which have the highest sensitivity to γ are all compatible with zero at the 2σ level. The correlations between $\mathcal{R}_{SS/OS}$ ratio and the ratios $\mathcal{R}_{DK/D\pi,SS}$ and $\mathcal{R}_{DK/D\pi,OS}$ are -16% (-13%) and $+16\%$ ($+16\%$), respectively, for the fit to the whole Dalitz plot ($K^*(892)^\pm$ region). The correlation between the $\mathcal{R}_{DK/D\pi,SS}$ and $\mathcal{R}_{DK/D\pi,OS}$ ratios is $+11\%$ ($+15\%$). Correlations between the asymmetry observables are all less than 1% and are neglected.

6. Systematic uncertainties

The largest single source of systematic uncertainty is the knowledge of the efficiency correction factor that multiplies the $\mathcal{R}_{SS/OS}$ observable. This uncertainty has three sources: the uncertainties on the CLEO amplitude models, the granularity of the Dalitz divisions in which the acceptance is determined, and the limited size of the simulated sample available to determine the LHCb acceptance. Of these, it is the modelling uncertainty that is dominant. In addition, an uncertainty is assigned to account for the fact that interference is neglected in the computation of the efficiency correction factor, which is shared between the $D\pi^\pm$ and $DK^\pm$ systems.

Uncertainties on the parameters that are fixed in the PDF are propagated to the observables by repeating the fit to data whilst

Table 3
Absolute values of systematic uncertainties, in units of 10^{-2}, for the fit to the whole Dalitz plot.

Observable	Eff. correction	Fit PDFs	Prod. and det. asymms.	PID	Total
$\mathcal{R}_{SS/OS}$	2.40	0.50	–	0.01	2.45
$\mathcal{R}_{DK/D\pi,SS}$	0.01	0.38	–	0.02	0.38
$\mathcal{R}_{DK/D\pi,OS}$	0.01	0.19	–	0.01	0.19
$\mathcal{A}_{SS,DK}$	0.14	0.44	1.71	0.01	1.78
$\mathcal{A}_{OS,DK}$	0.36	2.13	0.99	0.01	2.37
$\mathcal{A}_{SS,D\pi}$	0.02	0.05	0.99	< 0.01	0.99
$\mathcal{A}_{OS,D\pi}$	0.03	0.10	1.71	< 0.01	1.72

Table 4
Absolute values of systematic uncertainties, in units of 10^{-2}, for the fit in the restricted region.

Observable	Eff. correction	Fit PDFs	Prod. and det. asymms.	PID	Total
$\mathcal{R}_{SS/OS}$	6.08	0.53	–	0.01	6.10
$\mathcal{R}_{DK/D\pi,SS}$	0.01	0.25	–	0.02	0.25
$\mathcal{R}_{DK/D\pi,OS}$	0.01	0.21	–	0.01	0.21
$\mathcal{A}_{SS,DK}$	0.13	2.27	1.71	0.01	2.85
$\mathcal{A}_{OS,DK}$	0.04	2.38	0.99	0.01	2.57
$\mathcal{A}_{SS,D\pi}$	0.04	0.17	0.99	< 0.01	1.00
$\mathcal{A}_{OS,D\pi}$	0.06	0.09	1.71	< 0.01	1.72

varying each fixed parameter according to its uncertainty. An additional systematic uncertainty is calculated for the fit to the restricted $K^*(892)^\pm$ region, where the $D\pi^\pm$ combinatorial background slopes are fixed to the values determined in the fit to the whole Dalitz plot.

Uncertainties are assigned to account for the errors on the $B^\pm$ production asymmetry and the $K^\pm$ and $\pi^\pm$ detection asymmetries. The effect of the detection asymmetry depends on the pion and kaon content of the final state, and the resulting systematic uncertainty is largest for the $\mathcal{A}_{SS,DK}$ and $\mathcal{A}_{OS,D\pi}$ observables.

The absolute uncertainties on the particle identification efficiencies are small, typically around 0.3% for kaon efficiencies and 0.03% for pion efficiencies. Of the four main sources of systematic error, these result in the smallest uncertainties on the experimental observables.

In Table 3, the sources of systematic uncertainty are given for each observable in the fit to the whole Dalitz plot. Similarly those for the fit in the restricted region are given in Table 4.

7. Interpretation and conclusions

The sensitivity of this result to the CKM angle γ is investigated by employing a frequentist method to scan the $\gamma - r_B$ parameter space and calculate the χ^2 probability at each point, given the measurements of the observables with their statistical and systematic uncertainties combined in quadrature, accounting for correlations between the statistical uncertainties. The effects of charm mixing are accounted for, but *CP* violation in the decays of D mesons is neglected. Regions of 1σ, 2σ and 3σ compatibility with the measurements made are indicated by the dark, medium and light blue regions, respectively, in Fig. 4. The small sample size in the current data set results in a bound on γ that is only closed for the 1σ contour.

Although it is not possible to measure γ directly using these results alone, it is of interest to consider how this result relates to the previous LHCb γ determination, obtained from other $B^\pm \to DK^\pm$ modes [8], since it will be included in future combinations. In order to aid this comparison, the scans of the $\gamma - r_B$ space plots are shown in Fig. 4(a) for the measurement made using the whole $D \to K^0_S K\pi$ Dalitz plot and in Fig. 4(b) for that made in the restricted region. The current LHCb average, extracted from a combination of $B^\pm \to DK^\pm$ analyses [8], is shown as a point with error bars at $\gamma = 72.0^\circ$ and $r_B = 0.089$. The LHCb average lies within the 2σ region allowed by the measurements presented in this Letter. It is interesting to note that the bound determined in the $\gamma - r_B$ space indicates a more stringent constraint when using the restricted region, where the coherence is higher. This, and the fact that the measurements in this Letter are limited by their statistical precision, motivates the use of this region in future analyses of these decays in a larger data sample. Combination with analyses in other, more abundant channels with sensitivity to the same parameters will yield more stringent constraints upon γ.

In summary, for the first time a measurement of charge asymmetries and associated observables is presented in the decay modes $B^\pm \to [K^0_S K^\pm \pi^\mp]_D h^\pm$ and $B^\pm \to [K^0_S K^\mp \pi^\pm]_D h^\pm$, and no significant *CP* violation is observed. The results of the analysis are consistent with other measurements of observables in related $B^\pm \to DK^\pm$ modes, and will be valuable in future global fits of the CKM parameter γ.

Acknowledgements

We express our gratitude to our colleagues in the CERN accelerator departments for the excellent performance of the LHC. We thank the technical and administrative staff at the LHCb institutes. We acknowledge support from CERN and from the national agencies: CAPES, CNPq, FAPERJ and FINEP (Brazil); NSFC (China); CNRS/IN2P3 and Region Auvergne (France); BMBF, DFG, HGF and MPG (Germany); SFI (Ireland); INFN (Italy); FOM and NWO (The Netherlands); SCSR (Poland); MEN/IFA (Romania); MinES, Rosatom, RFBR and NRC "Kurchatov Institute" (Russia); MinECo, XuntaGal and GENCAT (Spain); SNSF and SER (Switzerland); NAS Ukraine

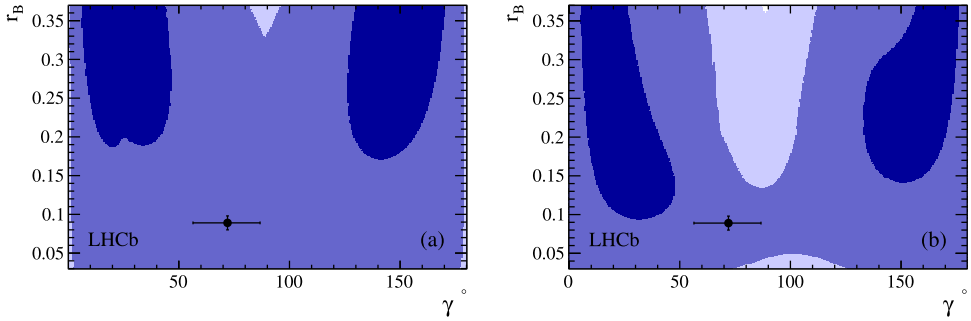

Fig. 4. Scans of the χ^2 probabilities over the $\gamma - r_B$ parameter space for (a) the whole Dalitz fit and (b) the fit inside the K^* region (b). The contours are the usual $n\sigma$ profile likelihood contours, where $\Delta\chi^2 = n^2$ with $n = 1$ (dark blue), 2 (medium blue), and 3 (light blue). The 2σ contour encloses almost all of the parameter space shown, so a central value of γ and relevant bounds are not extracted. The result is seen to be compatible with the current LHCb measurement of γ, indicated by the point at ($\gamma = 72.0^\circ$ and $r_B = 0.089$), at a level between 1 and 2σ.

(Ukraine); STFC (United Kingdom); NSF (USA). We also acknowledge the support received from the ERC under FP7. The Tier1 computing centres are supported by IN2P3 (France), KIT and BMBF (Germany), INFN (Italy), NWO and SURF (The Netherlands), PIC (Spain), GridPP (United Kingdom). We are indebted to the communities behind the multiple open source software packages we depend on. We are also thankful for the computing resources and the access to software R&D tools provided by Yandex LLC (Russia).

References

[1] M. Gronau, D. London, How to determine all the angles of the unitarity triangle from $B_d^0 \to DK_S^0$ and $B_s^0 \to D\phi$, Phys. Lett. B 253 (1991) 483.
[2] M. Gronau, D. Wyler, On determining a weak phase from charged B decay asymmetries, Phys. Lett. B 265 (1991) 172.
[3] D. Atwood, I. Dunietz, A. Soni, Enhanced CP violation with $B \to KD^0(\overline{D}^0)$ modes and extraction of the CKM angle γ, Phys. Rev. Lett. 78 (1997) 3257, arXiv:hep-ph/9612433.
[4] D. Atwood, I. Dunietz, A. Soni, Improved methods for observing CP violation in $B^\pm \to K^\pm D$ and measuring the CKM phase γ, Phys. Rev. D 63 (2001) 036005, arXiv:hep-ph/0008090.
[5] LHCb Collaboration, R. Aaij, et al., Observation of CP violation in $B^\pm \to DK^\pm$ decays, Phys. Lett. B 712 (2012) 203, arXiv:1203.3662.
[6] LHCb Collaboration, R. Aaij, et al., A model-independent Dalitz plot analysis of $B^\pm \to DK^\pm$ with $D \to K_S^0 h^+ h^-$ ($h = \pi, K$) decays and constraints on the CKM angle γ, Phys. Lett. B 718 (2012) 43, arXiv:1209.5869.
[7] LHCb Collaboration, R. Aaij, et al., Observation of the suppressed ADS modes $B^\pm \to [\pi^\pm K^\mp \pi^+ \pi^-]_D K^\pm$ and $B^\pm \to [\pi^\pm K^\mp \pi^+ \pi^-]_D \pi^\pm$, Phys. Lett. B 723 (2013) 44, arXiv:1303.4646.
[8] LHCb Collaboration, R. Aaij, et al., A measurement of γ from a combination of $B^\pm \to Dh^\pm$ analyses, Phys. Lett. B 726 (2013) 151, arXiv:1305.2050.
[9] BaBar Collaboration, J. Lees, et al., Observation of direct CP violation in the measurement of the Cabibbo–Kobayashi–Maskawa angle γ with $B^\pm \to D^{(*)} K^{(*)\pm}$ decays, Phys. Rev. D 87 (2013) 052015, arXiv:1301.1029.
[10] Belle Collaboration, K. Trabelsi, Study of direct CP in charmed B decays and measurement of the CKM angle gamma at Belle, arXiv:1301.2033, presented at CKM2012, Cincinnati, USA, 28 September–2 October 2012.
[11] LHCb Collaboration, R. Aaij, et al., Measurement of CP observables in $B^0 \to DK^{*0}$ with $D \to K^+K^-$, J. High Energy Phys. 1303 (2013) 67, arXiv:1212.5205.
[12] CLEO Collaboration, J. Insler, et al., Studies of the decays $D^0 \to K_S^0 K^-\pi^+$ and $D^0 \to K_S^0 K^+\pi^-$, Phys. Rev. D 85 (2012) 092016, arXiv:1203.3804.
[13] D. Atwood, A. Soni, Role of a charm factory in extracting CKM-phase information via $B \to DK$, Phys. Rev. D 68 (2003) 033003, arXiv:hep-ph/0304085.
[14] LHCb Collaboration, A.A. Alves Jr., et al., The LHCb detector at the LHC, J. Instrum. 3 (2008) S08005.
[15] M. Adinolfi, et al., Performance of the LHCb RICH detector at the LHC, Eur. Phys. J. C 73 (2013) 2431, arXiv:1211.6759.
[16] V.V. Gligorov, M. Williams, Efficient, reliable and fast high-level triggering using a bonsai boosted decision tree, J. Instrum. 8 (2013) P02013, arXiv:1210.6861.
[17] T. Sjöstrand, S. Mrenna, P. Skands, PYTHIA 6.4 physics and manual, J. High Energy Phys. 0605 (2006) 026, arXiv:hep-ph/0603175;
T. Sjöstrand, S. Mrenna, P. Skands, A brief introduction to PYTHIA 8.1, Comput. Phys. Commun. 178 (2008) 852, arXiv:0710.3820.
[18] I. Belyaev, et al., Handling of the generation of primary events in Gauss, the LHCb simulation framework, in: Nuclear Science Symposium Conference Record, NSS/MIC, IEEE, 2010, p. 1155.
[19] D.J. Lange, The EvtGen particle decay simulation package, Nucl. Instrum. Methods A 462 (2001) 152.
[20] P. Golonka, Z. Was, PHOTOS Monte Carlo: a precision tool for QED corrections in Z and W decays, Eur. Phys. J. C 45 (2006) 97, arXiv:hep-ph/0506026.
[21] Geant4 Collaboration, J. Allison, et al., Geant4 developments and applications, IEEE Trans. Nucl. Sci. 53 (2006) 270;
Geant4 Collaboration, S. Agostinelli, et al., Geant4: a simulation toolkit, Nucl. Instrum. Methods A 506 (2003) 250.
[22] M. Clemencic, et al., The LHCb simulation application, Gauss: design, evolution and experience, J. Phys. Conf. Ser. 331 (2011) 032023.
[23] Particle Data Group, J. Beringer, et al., Review of particle physics, Phys. Rev. D 86 (2012) 010001, and 2013 partial update for the 2014 edition.
[24] W.D. Hulsbergen, Decay chain fitting with a Kalman filter, Nucl. Instrum. Methods, Sect. A 552 (2005) 566, arXiv:physics/0503191.
[25] L. Breiman, J.H. Friedman, R.A. Olshen, C.J. Stone, Classification and Regression Trees, Wadsworth International Group, Belmont, California, USA, 1984.
[26] R.E. Schapire, Y. Freund, A decision-theoretic generalization of on-line learning and an application to boosting, J. Comput. Syst. Sci. 55 (1997) 119.
[27] T. Skwarnicki, A study of the radiative cascade transitions between the Upsilon-prime and Upsilon resonances, PhD thesis, Institute of Nuclear Physics, Krakow, 1986.
[28] LHCb Collaboration, R. Aaij, et al., Measurements of the branching fractions and CP asymmetries of $B^\pm \to J/\psi\pi^\pm$ and $B^\pm \to \psi(2S)\pi^\pm$ decays, Phys. Rev. D 85 (2012) 091105(R), arXiv:1203.3592.

LHCb Collaboration

R. Aaij [41], B. Adeva [37], M. Adinolfi [46], A. Affolder [52], Z. Ajaltouni [5], J. Albrecht [9], F. Alessio [38], M. Alexander [51], S. Ali [41], G. Alkhazov [30], P. Alvarez Cartelle [37], A.A. Alves Jr [25], S. Amato [2], S. Amerio [22], Y. Amhis [7], L. Anderlini [17,g], J. Anderson [40], R. Andreassen [57], M. Andreotti [16,f], J.E. Andrews [58], R.B. Appleby [54], O. Aquines Gutierrez [10], F. Archilli [38], A. Artamonov [35], M. Artuso [59], E. Aslanides [6], G. Auriemma [25,n], M. Baalouch [5], S. Bachmann [11], J.J. Back [48], A. Badalov [36], V. Balagura [31], W. Baldini [16], R.J. Barlow [54], C. Barschel [39], S. Barsuk [7], W. Barter [47], V. Batozskaya [28], Th. Bauer [41], A. Bay [39], J. Beddow [51], F. Bedeschi [23], I. Bediaga [1], S. Belogurov [31], K. Belous [35], I. Belyaev [31], E. Ben-Haim [8], G. Bencivenni [18], S. Benson [50], J. Benton [46], A. Berezhnoy [32], R. Bernet [40], M.-O. Bettler [47], M. van Beuzekom [41], A. Bien [11], S. Bifani [45], T. Bird [54], A. Bizzeti [17,i], P.M. Bjørnstad [54], T. Blake [48], F. Blanc [39], J. Blouw [10], S. Blusk [59], V. Bocci [25], A. Bondar [34,66], N. Bondar [30], W. Bonivento [15,38], S. Borghi [54], A. Borgia [59], M. Borsato [7], T.J.V. Bowcock [52], E. Bowen [40], C. Bozzi [16], T. Brambach [9], J. van den Brand [42], J. Bressieux [39], D. Brett [54], M. Britsch [10], T. Britton [59], N.H. Brook [46], H. Brown [52], A. Bursche [40], G. Busetto [22,r], J. Buytaert [38], S. Cadeddu [15], R. Calabrese [16,f], O. Callot [7], M. Calvi [20,k], M. Calvo Gomez [36,p], A. Camboni [36], P. Campana [18,38], D. Campora Perez [38], A. Carbone [14,d], G. Carboni [24,l], R. Cardinale [19,j], A. Cardini [15], H. Carranza-Mejia [50], L. Carson [50], K. Carvalho Akiba [2], G. Casse [52], L. Cassina [20], L. Castillo Garcia [38], M. Cattaneo [38], Ch. Cauet [9], R. Cenci [58], M. Charles [8], Ph. Charpentier [38], S.-F. Cheung [55], N. Chiapolini [40], M. Chrzaszcz [40,26], K. Ciba [38], X. Cid Vidal [38], G. Ciezarek [53], P.E.L. Clarke [50], M. Clemencic [38], H.V. Cliff [47], J. Closier [38], C. Coca [29], V. Coco [38], J. Cogan [6], E. Cogneras [5], P. Collins [38], A. Comerma-Montells [36], A. Contu [15,38], A. Cook [46], M. Coombes [46], S. Coquereau [8], G. Corti [38], I. Counts [56], B. Couturier [38], G.A. Cowan [50], D.C. Craik [48], M. Cruz Torres [60], S. Cunliffe [53], R. Currie [50], C. D'Ambrosio [38], J. Dalseno [46], P. David [8], P.N.Y. David [41], A. Davis [57], I. De Bonis [4], K. De Bruyn [41], S. De Capua [54], M. De Cian [11], J.M. De Miranda [1], L. De Paula [2],

W. De Silva [57], P. De Simone [18], D. Decamp [4], M. Deckenhoff [9], L. Del Buono [8], N. Déléage [4], D. Derkach [55], O. Deschamps [5], F. Dettori [42], A. Di Canto [11], H. Dijkstra [38], S. Donleavy [52], F. Dordei [11], M. Dorigo [39], P. Dorosz [26,o], A. Dosil Suárez [37], D. Dossett [48], A. Dovbnya [43], F. Dupertuis [39], P. Durante [38], R. Dzhelyadin [35], A. Dziurda [26], A. Dzyuba [30], S. Easo [49], U. Egede [53], V. Egorychev [31], S. Eidelman [34,66], S. Eisenhardt [50], U. Eitschberger [9], R. Ekelhof [9], L. Eklund [51,38], I. El Rifai [5], Ch. Elsasser [40], S. Esen [11], A. Falabella [16,f], C. Färber [11], C. Farinelli [41], S. Farry [52], D. Ferguson [50], V. Fernandez Albor [37], F. Ferreira Rodrigues [1], M. Ferro-Luzzi [38], S. Filippov [33], M. Fiore [16,f], M. Fiorini [16,f], C. Fitzpatrick [38], M. Fontana [10], F. Fontanelli [19,j], R. Forty [38], O. Francisco [2], M. Frank [38], C. Frei [38], M. Frosini [17,38,g], J. Fu [21], E. Furfaro [24,l], A. Gallas Torreira [37], D. Galli [14,d], M. Gandelman [2], P. Gandini [59], Y. Gao [3], J. Garofoli [59], J. Garra Tico [47], L. Garrido [36], C. Gaspar [38], R. Gauld [55], L. Gavardi [9], E. Gersabeck [11], M. Gersabeck [54], T. Gershon [48], Ph. Ghez [4], A. Gianelle [22], S. Giani' [39], V. Gibson [47], L. Giubega [29], V.V. Gligorov [38], C. Göbel [60], D. Golubkov [31], A. Golutvin [53,31,38], A. Gomes [1,a], H. Gordon [38], M. Grabalosa Gándara [5], R. Graciani Diaz [36], L.A. Granado Cardoso [38], E. Graugés [36], G. Graziani [17], A. Grecu [29], E. Greening [55], S. Gregson [47], P. Griffith [45], L. Grillo [11], O. Grünberg [61], B. Gui [59], E. Gushchin [33], Yu. Guz [35,38], T. Gys [38], C. Hadjivasiliou [59], G. Haefeli [39], C. Haen [38], T.W. Hafkenscheid [64], S.C. Haines [47], S. Hall [53], B. Hamilton [58], T. Hampson [46], S. Hansmann-Menzemer [11], N. Harnew [55], S.T. Harnew [46], J. Harrison [54], T. Hartmann [61], J. He [38], T. Head [38], V. Heijne [41], K. Hennessy [52], P. Henrard [5], L. Henry [8], J.A. Hernando Morata [37], E. van Herwijnen [38], M. Heß [61], A. Hicheur [1], D. Hill [55], M. Hoballah [5], C. Hombach [54], W. Hulsbergen [41], P. Hunt [55], N. Hussain [55], D. Hutchcroft [52], D. Hynds [51], V. Iakovenko [44], M. Idzik [27], P. Ilten [56], R. Jacobsson [38], A. Jaeger [11], E. Jans [41], P. Jaton [39], A. Jawahery [58], F. Jing [3], M. John [55], D. Johnson [55,*], C.R. Jones [47], C. Joram [38], B. Jost [38], N. Jurik [59], M. Kaballo [9], S. Kandybei [43], W. Kanso [6], M. Karacson [38], T.M. Karbach [38], M. Kelsey [59], I.R. Kenyon [45], T. Ketel [42], B. Khanji [20], C. Khurewathanakul [39], S. Klaver [54], O. Kochebina [7], I. Komarov [39], R.F. Koopman [42], P. Koppenburg [41], M. Korolev [32], A. Kozlinskiy [41], L. Kravchuk [33], K. Kreplin [11], M. Kreps [48], G. Krocker [11], P. Krokovny [34,66], F. Kruse [9], M. Kucharczyk [20,26,38,k], V. Kudryavtsev [34,66], K. Kurek [28], T. Kvaratskheliya [31,38], V.N. La Thi [39], D. Lacarrere [38], G. Lafferty [54], A. Lai [15], D. Lambert [50], R.W. Lambert [42], E. Lanciotti [38], G. Lanfranchi [18], C. Langenbruch [38], T. Latham [48], C. Lazzeroni [45], R. Le Gac [6], J. van Leerdam [41], J.-P. Lees [4], R. Lefèvre [5], A. Leflat [32], J. Lefrançois [7], S. Leo [23], O. Leroy [6], T. Lesiak [26], B. Leverington [11], Y. Li [3], M. Liles [52], R. Lindner [38], C. Linn [38], F. Lionetto [40], B. Liu [15], G. Liu [38], S. Lohn [38], I. Longstaff [51], J.H. Lopes [2], N. Lopez-March [39], P. Lowdon [40], H. Lu [3], D. Lucchesi [22,r], J. Luisier [39], H. Luo [50], E. Luppi [16,f], O. Lupton [55], F. Machefert [7], I.V. Machikhiliyan [31], F. Maciuc [29], O. Maev [30,38], S. Malde [55], G. Manca [15,e], G. Mancinelli [6], M. Manzali [16,f], J. Maratas [5], U. Marconi [14], P. Marino [23,t], R. Märki [39], J. Marks [11], G. Martellotti [25], A. Martens [8], A. Martín Sánchez [7], M. Martinelli [41], D. Martinez Santos [42], F. Martinez Vidal [63], D. Martins Tostes [2], A. Massafferri [1], R. Matev [38], Z. Mathe [38], C. Matteuzzi [20], A. Mazurov [16,38,f], M. McCann [53], J. McCarthy [45], A. McNab [54], R. McNulty [12], B. McSkelly [52], B. Meadows [57,55], F. Meier [9], M. Meissner [11], M. Merk [41], D.A. Milanes [8], M.-N. Minard [4], J. Molina Rodriguez [60], S. Monteil [5], D. Moran [54], M. Morandin [22], P. Morawski [26], A. Mordà [6], M.J. Morello [23,t], R. Mountain [59], F. Muheim [50], K. Müller [40], R. Muresan [29], B. Muryn [27], B. Muster [39], P. Naik [46], T. Nakada [39], R. Nandakumar [49], I. Nasteva [1], M. Needham [50], N. Neri [21], S. Neubert [38], N. Neufeld [38], A.D. Nguyen [39], T.D. Nguyen [39], C. Nguyen-Mau [39,q], M. Nicol [7], V. Niess [5], R. Niet [9], N. Nikitin [32], T. Nikodem [11], A. Novoselov [35], A. Oblakowska-Mucha [27], V. Obraztsov [35], S. Oggero [41], S. Ogilvy [51], O. Okhrimenko [44], R. Oldeman [15,e], G. Onderwater [64], M. Orlandea [29], J.M. Otalora Goicochea [2], P. Owen [53], A. Oyanguren [36], B.K. Pal [59], A. Palano [13,c], F. Palombo [21,u], M. Palutan [18], J. Panman [38], A. Papanestis [49,38], M. Pappagallo [51], L. Pappalardo [16], C. Parkes [54], C.J. Parkinson [9], G. Passaleva [17], G.D. Patel [52], M. Patel [53], C. Patrignani [19,j], C. Pavel-Nicorescu [29], A. Pazos Alvarez [37], A. Pearce [54], A. Pellegrino [41], G. Penso [25,m], M. Pepe Altarelli [38], S. Perazzini [14,d], E. Perez Trigo [37], P. Perret [5], M. Perrin-Terrin [6], L. Pescatore [45], E. Pesen [65], G. Pessina [20], K. Petridis [53], A. Petrolini [19,j], E. Picatoste Olloqui [36], B. Pietrzyk [4], T. Pilař [48], D. Pinci [25], A. Pistone [19], S. Playfer [50], M. Plo Casasus [37], F. Polci [8], G. Polok [26], A. Poluektov [48,34], E. Polycarpo [2], A. Popov [35], D. Popov [10], B. Popovici [29], C. Potterat [36], A. Powell [55], J. Prisciandaro [39], A. Pritchard [52], C. Prouve [46], V. Pugatch [44], A. Puig Navarro [39], G. Punzi [23,s], W. Qian [4], B. Rachwal [26], J.H. Rademacker [46], B. Rakotomiaramanana [39], M. Rama [18], M.S. Rangel [2], I. Raniuk [43], N. Rauschmayr [38], G. Raven [42], S. Redford [55], S. Reichert [54], M.M. Reid [48], A.C. dos Reis [1], S. Ricciardi [49], A. Richards [53], K. Rinnert [52],

V. Rives Molina [36], D.A. Roa Romero [5], P. Robbe [7], D.A. Roberts [58], A.B. Rodrigues [1], E. Rodrigues [54], P. Rodriguez Perez [37], S. Roiser [38], V. Romanovsky [35], A. Romero Vidal [37], M. Rotondo [22], J. Rouvinet [39], T. Ruf [38], F. Ruffini [23], H. Ruiz [36], P. Ruiz Valls [36], G. Sabatino [25,l], J.J. Saborido Silva [37], N. Sagidova [30], P. Sail [51], B. Saitta [15,e], V. Salustino Guimaraes [2], B. Sanmartin Sedes [37], R. Santacesaria [25], C. Santamarina Rios [37], E. Santovetti [24,l], M. Sapunov [6], A. Sarti [18], C. Satriano [25,n], A. Satta [24], M. Savrie [16,f], D. Savrina [31,32], M. Schiller [42], H. Schindler [38], M. Schlupp [9], M. Schmelling [10], B. Schmidt [38], O. Schneider [39], A. Schopper [38], M.-H. Schune [7], R. Schwemmer [38], B. Sciascia [18], A. Sciubba [25], M. Seco [37], A. Semennikov [31], K. Senderowska [27], I. Sepp [53], N. Serra [40], J. Serrano [6], P. Seyfert [11], M. Shapkin [35], I. Shapoval [16,43,f], Y. Shcheglov [30], T. Shears [52], L. Shekhtman [34,66], O. Shevchenko [43], V. Shevchenko [62], A. Shires [9], R. Silva Coutinho [48], G. Simi [22], M. Sirendi [47], N. Skidmore [46], T. Skwarnicki [59], N.A. Smith [52], E. Smith [55,49], E. Smith [53], J. Smith [47], M. Smith [54], H. Snoek [41], M.D. Sokoloff [57], F.J.P. Soler [51], F. Soomro [39], D. Souza [46], B. Souza De Paula [2], B. Spaan [9], A. Sparkes [50], F. Spinella [23], P. Spradlin [51], F. Stagni [38], S. Stahl [11], O. Steinkamp [40], S. Stevenson [55], S. Stoica [29], S. Stone [59], B. Storaci [40], S. Stracka [23,38], M. Straticiuc [29], U. Straumann [40], R. Stroili [22], V.K. Subbiah [38], L. Sun [57], W. Sutcliffe [53], S. Swientek [9], V. Syropoulos [42], M. Szczekowski [28], P. Szczypka [39,38], D. Szilard [2], T. Szumlak [27], S. T'Jampens [4], M. Teklishyn [7], G. Tellarini [16,f], E. Teodorescu [29], F. Teubert [38], C. Thomas [55], E. Thomas [38], J. van Tilburg [11], V. Tisserand [4], M. Tobin [39], S. Tolk [42], L. Tomassetti [16,f], D. Tonelli [38], S. Topp-Joergensen [55], N. Torr [55], E. Tournefier [4,53], S. Tourneur [39], M.T. Tran [39], M. Tresch [40], A. Tsaregorodtsev [6], P. Tsopelas [41], N. Tuning [41], M. Ubeda Garcia [38], A. Ukleja [28], A. Ustyuzhanin [62], U. Uwer [11], V. Vagnoni [14], G. Valenti [14], A. Vallier [7], R. Vazquez Gomez [18], P. Vazquez Regueiro [37], C. Vázquez Sierra [37], S. Vecchi [16], J.J. Velthuis [46], M. Veltri [17,h], G. Veneziano [39], M. Vesterinen [11], B. Viaud [7], D. Vieira [2], X. Vilasis-Cardona [36,p], A. Vollhardt [40], D. Volyanskyy [10], D. Voong [46], A. Vorobyev [30], V. Vorobyev [34,66], C. Voß [61], H. Voss [10], J.A. de Vries [41], R. Waldi [61], C. Wallace [48], R. Wallace [12], S. Wandernoth [11], J. Wang [59], D.R. Ward [47], N.K. Watson [45], A.D. Webber [54], D. Websdale [53], M. Whitehead [48], J. Wicht [38], J. Wiechczynski [26], D. Wiedner [11], L. Wiggers [41], G. Wilkinson [55], M.P. Williams [48,49], M. Williams [56], F.F. Wilson [49], J. Wimberley [58], J. Wishahi [9], W. Wislicki [28], M. Witek [26], G. Wormser [7], S.A. Wotton [47], S. Wright [47], S. Wu [3], K. Wyllie [38], Y. Xie [50,38], Z. Xing [59], Z. Yang [3], X. Yuan [3], O. Yushchenko [35], M. Zangoli [14], M. Zavertyaev [10,b], F. Zhang [3], L. Zhang [59], W.C. Zhang [12], Y. Zhang [3], A. Zhelezov [11], A. Zhokhov [31], L. Zhong [3], A. Zvyagin [38]

[1] *Centro Brasileiro de Pesquisas Físicas (CBPF), Rio de Janeiro, Brazil*
[2] *Universidade Federal do Rio de Janeiro (UFRJ), Rio de Janeiro, Brazil*
[3] *Center for High Energy Physics, Tsinghua University, Beijing, China*
[4] *LAPP, Université de Savoie, CNRS/IN2P3, Annecy-Le-Vieux, France*
[5] *Clermont Université, Université Blaise Pascal, CNRS/IN2P3, LPC, Clermont-Ferrand, France*
[6] *CPPM, Aix-Marseille Université, CNRS/IN2P3, Marseille, France*
[7] *LAL, Université Paris-Sud, CNRS/IN2P3, Orsay, France*
[8] *LPNHE, Université Pierre et Marie Curie, Université Paris Diderot, CNRS/IN2P3, Paris, France*
[9] *Fakultät Physik, Technische Universität Dortmund, Dortmund, Germany*
[10] *Max-Planck-Institut für Kernphysik (MPIK), Heidelberg, Germany*
[11] *Physikalisches Institut, Ruprecht-Karls-Universität Heidelberg, Heidelberg, Germany*
[12] *School of Physics, University College Dublin, Dublin, Ireland*
[13] *Sezione INFN di Bari, Bari, Italy*
[14] *Sezione INFN di Bologna, Bologna, Italy*
[15] *Sezione INFN di Cagliari, Cagliari, Italy*
[16] *Sezione INFN di Ferrara, Ferrara, Italy*
[17] *Sezione INFN di Firenze, Firenze, Italy*
[18] *Laboratori Nazionali dell'INFN di Frascati, Frascati, Italy*
[19] *Sezione INFN di Genova, Genova, Italy*
[20] *Sezione INFN di Milano Bicocca, Milano, Italy*
[21] *Sezione INFN di Milano, Milano, Italy*
[22] *Sezione INFN di Padova, Padova, Italy*
[23] *Sezione INFN di Pisa, Pisa, Italy*
[24] *Sezione INFN di Roma Tor Vergata, Roma, Italy*
[25] *Sezione INFN di Roma La Sapienza, Roma, Italy*
[26] *Henryk Niewodniczanski Institute of Nuclear Physics Polish Academy of Sciences, Kraków, Poland*
[27] *AGH – University of Science and Technology, Faculty of Physics and Applied Computer Science, Kraków, Poland*
[28] *National Center for Nuclear Research (NCBJ), Warsaw, Poland*
[29] *Horia Hulubei National Institute of Physics and Nuclear Engineering, Bucharest-Magurele, Romania*
[30] *Petersburg Nuclear Physics Institute (PNPI), Gatchina, Russia*
[31] *Institute of Theoretical and Experimental Physics (ITEP), Moscow, Russia*
[32] *Institute of Nuclear Physics, Moscow State University (SINP MSU), Moscow, Russia*
[33] *Institute for Nuclear Research of the Russian Academy of Sciences (INR RAN), Moscow, Russia*
[34] *Budker Institute of Nuclear Physics (SB RAS), Russia*

[35] Institute for High Energy Physics (IHEP), Protvino, Russia
[36] Universitat de Barcelona, Barcelona, Spain
[37] Universidad de Santiago de Compostela, Santiago de Compostela, Spain
[38] European Organization for Nuclear Research (CERN), Geneva, Switzerland
[39] Ecole Polytechnique Fédérale de Lausanne (EPFL), Lausanne, Switzerland
[40] Physik-Institut, Universität Zürich, Zürich, Switzerland
[41] Nikhef National Institute for Subatomic Physics, Amsterdam, The Netherlands
[42] Nikhef National Institute for Subatomic Physics and VU University Amsterdam, Amsterdam, The Netherlands
[43] NSC Kharkiv Institute of Physics and Technology (NSC KIPT), Kharkiv, Ukraine
[44] Institute for Nuclear Research of the National Academy of Sciences (KINR), Kyiv, Ukraine
[45] University of Birmingham, Birmingham, United Kingdom
[46] H.H. Wills Physics Laboratory, University of Bristol, Bristol, United Kingdom
[47] Cavendish Laboratory, University of Cambridge, Cambridge, United Kingdom
[48] Department of Physics, University of Warwick, Coventry, United Kingdom
[49] STFC Rutherford Appleton Laboratory, Didcot, United Kingdom
[50] School of Physics and Astronomy, University of Edinburgh, Edinburgh, United Kingdom
[51] School of Physics and Astronomy, University of Glasgow, Glasgow, United Kingdom
[52] Oliver Lodge Laboratory, University of Liverpool, Liverpool, United Kingdom
[53] Imperial College London, London, United Kingdom
[54] School of Physics and Astronomy, University of Manchester, Manchester, United Kingdom
[55] Department of Physics, University of Oxford, Oxford, United Kingdom
[56] Massachusetts Institute of Technology, Cambridge, MA, United States
[57] University of Cincinnati, Cincinnati, OH, United States
[58] University of Maryland, College Park, MD, United States
[59] Syracuse University, Syracuse, NY, United States
[60] Pontifícia Universidade Católica do Rio de Janeiro (PUC-Rio), Rio de Janeiro, Brazil [v]
[61] Institut für Physik, Universität Rostock, Rostock, Germany [w]
[62] National Research Centre Kurchatov Institute, Moscow, Russia [x]
[63] Instituto de Fisica Corpuscular (IFIC), Universitat de Valencia-CSIC, Valencia, Spain [y]
[64] KVI-University of Groningen, Groningen, The Netherlands [z]
[65] Celal Bayar University, Manisa, Turkey [aa]
[66] Novosibirsk State University, Novosibirsk, Russia

* Corresponding author.
[a] Universidade Federal do Triângulo Mineiro (UFTM), Uberaba-MG, Brazil.
[b] P.N. Lebedev Physical Institute, Russian Academy of Science (LPI RAS), Moscow, Russia.
[c] Università di Bari, Bari, Italy.
[d] Università di Bologna, Bologna, Italy.
[e] Università di Cagliari, Cagliari, Italy.
[f] Università di Ferrara, Ferrara, Italy.
[g] Università di Firenze, Firenze, Italy.
[h] Università di Urbino, Urbino, Italy.
[i] Università di Modena e Reggio Emilia, Modena, Italy.
[j] Università di Genova, Genova, Italy.
[k] Università di Milano Bicocca, Milano, Italy.
[l] Università di Roma Tor Vergata, Roma, Italy.
[m] Università di Roma La Sapienza, Roma, Italy.
[n] Università della Basilicata, Potenza, Italy.
[o] AGH – University of Science and Technology, Faculty of Computer Science, Electronics and Telecommunications, Kraków, Poland.
[p] LIFAELS, La Salle, Universitat Ramon Llull, Barcelona, Spain.
[q] Hanoi University of Science, Hanoi, Viet Nam.
[r] Università di Padova, Padova, Italy.
[s] Università di Pisa, Pisa, Italy.
[t] Scuola Normale Superiore, Pisa, Italy.
[u] Università degli Studi di Milano, Milano, Italy.
[v] Associated to Universidade Federal do Rio de Janeiro (UFRJ), Rio de Janeiro, Brazil.
[w] Associated to Physikalisches Institut, Ruprecht-Karls-Universität Heidelberg, Heidelberg, Germany.
[x] Associated to Institute of Theoretical and Experimental Physics (ITEP), Moscow, Russia.
[y] Associated to Universitat de Barcelona, Barcelona, Spain.
[z] Associated to Nikhef National Institute for Subatomic Physics, Amsterdam, The Netherlands.
[aa] Associated to European Organization for Nuclear Research (CERN), Geneva, Switzerland.